38th International Electric Vehicle Symposium and Exhibition (EVS38) Göteborg, Sweden, June 15-18, 2025

Experimental research of proton exchange membrane fuel cells considering operating conditions and temperature

Shengxiang Fu[1,2], Dongeon Kim[1], Minsu Kim[1], Chunhua Zheng[2], Heeyun Lee[3], Namwook Kim[1*]

[1]*Department of Mechanical Engineering, BK21 FOUR ERICA-ACE Center, Hanyang University, Ansan, Gyeonggi 15588, Republic of Korea (nwkim@hanyang.ac.kr)*

[2]*Shenzhen Institutes of Advanced Technology, Chinese Academy of Sciences, Shenzhen 518055, China (ch.zheng@siat.ac.cn)*

[3]*Department of Mechanical Engineering, Dankook University, Yongin, Gyeonggi 16890, Republic of Korea (heeyunlee@dankook.ac.kr)*

Abstract

In order to explore the influence of the operating condition and temperature for proton exchange membrane fuel cells (PEMFCs), a voltage-based PEMFC stack test is developed in this study. The operating condition consists of idling, high-power, load-changing, and start-stop, and the test temperature is set as [60, 65, 70, 75, 80, 85] ℃ respectively. For a comprehensive analysis, a linear regression model is employed to quantify performance decline, while cell voltage monitoring (CVM) consistency serves as an index for assessing internal stack condition variations. Results show that temperature significantly impacts the durability of the PEMFC across different vehicle operating conditions.

Keywords: Proton exchange membrane fuel cell, Operating condition, Temperature, Linear regression, Cell voltage monitoring

1 Introduction

Proton exchange membrane fuel cells (PEMFCs) hold great application potential for the advantages of high energy conversion efficiency, high reliability, and zero-emission [1]. However, the severe operating conditions will cause difficulty in controlling the fuel cell system and aggravate the degradation eventually when the PEMFC is applied in automotive applications. In addition, the temperature also affects the durability of the PEMFC [2], where the higher temperature will lead to increasing evaporation of the liquid water while the lower temperature may cause the flooding of the cathode flow channel [3]. Considering the relationship between PEMFC durability and cost, it is necessary to evaluate the influence of the PEMFC under various operating conditions and temperatures simultaneously.

There are various theoretical and experimental approaches to examine and substantiate the relationship between operating conditions and internal electrochemical changes [4]-[9]. Research [10] summarized the typical operating conditions consisting of idling, high-power, load-changing, and start-stop as the main operating conditions for PEMFC degradation. The idling condition represents a prolonged low-current operation, which will induce high cathode-side potentials [6] and subsequently cause catalyst coarsening and

carbon corrosion in the gas diffusion electrode [7], [8]. On the contrary, the high-power condition usually occurs in the climbing and acceleration stages of automotive applications, and some phenomena such as air shortage [11], [12], flooding [13], local overheating [14], [15] are prone to appear in this period. The load-changing is regarded as the major condition in PEMFC performance degradation [16], where the electrochemically generated water and heat will create a warm and humid environment inside a PEMFC stack and accelerate the membrane and catalyst degradation. Furthermore, the load-changing condition also causes control difficulty in supply gas stoichiometry, temperature, pressure, and relative humidity. During the start-stop process, the hydrogen and oxygen may be present at the anode or cathode concurrently, the direct reaction of them would induce a huge potential difference (up to 1.5V) to cause the carbon carrier to be oxidized and corroded [17].

Since the typical operating conditions of PEMFC stacks inherently lead to variations in operating temperature, some studies take this factor into account. Research [18] conducted accelerated durability testing of PEMFC stacks under varying temperatures (60-85°C), where the PEMFC exhibits a maximum efficiency degradation of 14.7% under non-optimal thermal conditions. Research [19] conducted comparative durability testing at 55℃ and 70℃ on automotive PEMFC stacks. The findings demonstrate significantly better performance recovery effectiveness at 55℃ compared to only 4% recovery after 300 hours at 75℃. Furthermore, several temperature control methodologies have been adopted for the PEMFC stack in automotive applications. In reference [20], researchers implemented a PI-based thermal management system to regulate the inlet-outlet temperature change in a PEMFC stack, then the developed model was integrated into the Amesim platform. In addition, an artificial intelligence thermal control method was applied to regulate PEMFC stack temperatures, where the proposed method was validated through a fuel cell vehicle model from Autonomie software under comprehensive operating condition simulations [2]. However, there are limited research cases in comprehensive assessments simultaneously evaluating temperatures and operation conditions on the durability of PEMFC. Furthermore, the stack voltage uniformity during operation has received insufficient attention in most existing research.

According to the experimental protocol GB/T 24554-2022 standards [21], a voltage-based PEMFC test is developed in this study, where four operating conditions including idling, high-power, load-changing, and start-stop while the tests are processed under six temperatures [60, 65, 70, 75, 80, 85] ℃ respectively. To analyze the experiment results, a linear regression model is employed to quantify performance decline, and the cell voltage monitoring (CVM) consistency is set as an index for assessing internal condition variations of the stack. This research can systematically investigate the synergistic influences of operating conditions and temperature on PEMFC durability.

2 Experiment

2.1 Test Bench and PEMFC Stack

Figure 1 presents the 2kW test bench and the PEMFC stack of the test. The PEMFC stack utilizes the water-cooling method to control temperature, the specific parameter values of which are provided in Table 1. Before the operating condition test, the polarization test is processed to obtain the idling current, reference current, and rated current required for the operating condition test.

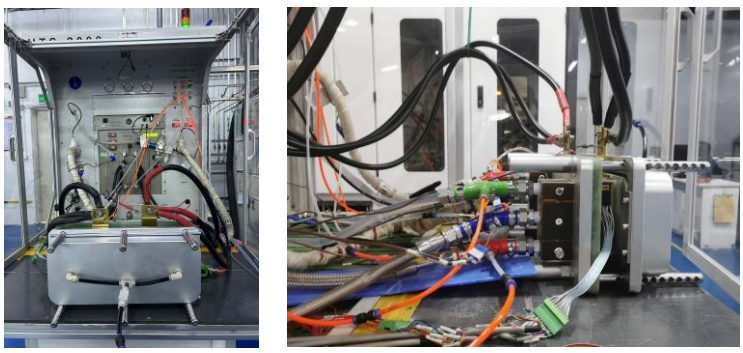

(a) (b)

Figure 1: Test system of PEMFC: (a) 2kW test bench, (b) PEMFC stack.

Table 1 Specific parameter values of PEMFC stack

Parameter	Value
Rated power (kW)	1.35
Cell number of the stack	9
Membrane thickness (cm)	0.0178
Cell active area (cm^2)	266

2.2 Operating condition Test

In this study, four typical operating condition tests including idling, high-power, load-changing, and start-stop are processed by adjusting the input current, where the idling, reference, and rated currents are determined through polarization testing. The load patterns are repeated to collect data from initial to final cycles, where the voltage values are measured under the reference current. Each long cycle comprises multiple short cycles, and there is a 1-hour stop following every long cycle. Besides, the tests are performed across temperatures of [60, 65, 70, 75, 80, 85] ℃ respectively to enable a comprehensive assessment of both operation conditions and temperatures on PEMFC durability.

2.2.1 Idling

For the idling condition, the test maintains the idling current for 3600 seconds first, then the load is switched to the reference current for voltage measurement. Subsequently, the load is reduced back to the idling current and marking the start of the next cycle. Figure 2 (a) presents the test trajectory for the idling condition test. Each long cycle consists of four such repeated cycles, and the test completes 5 long cycles at each specified temperature.

2.2.2 High-power

The rated current is set as the high-power condition in the proposed test. The procedure begins by maintaining the idling current for 90 seconds, then the stack load is switched to the rated current for 3600 seconds. In the next step, the load is reduced to the reference current for voltage measurement before returning directly to the rated current to initiate the next cycle. Figure 2 (b) presents the test trajectory for the high-power condition test. Each long cycle consists of four such repeated cycles, and the test completes 5 long cycles at each specified temperature.

2.2.3 Load-changing

The load-changing condition test indicates the change from the idling current to the rated current in this study. Firstly, the load is to maintain the idling current for 240s. Then the stack is loaded to the rated current for 3s and reduced to the idling current for 15s in the next step. The small cycle is repeated 216 times and after this, the stack is loaded to the reference current to measure the voltage. Figure 2 (c) presents the test trajectory of the load-changing condition, and the test completes 5 long cycles at each specified temperature.

2.2.4 Start-stop

The start-stop condition test follows the same loading pattern as the load-changing condition test, where the difference is that the long cycle of the start-stop condition test only consists of 27 short cycles and the voltage is measured after 8 long cycles. Figure 2 (d) presents the test trajectory of the start-stop condition, and the test completes 40 long cycles at each specified temperature.

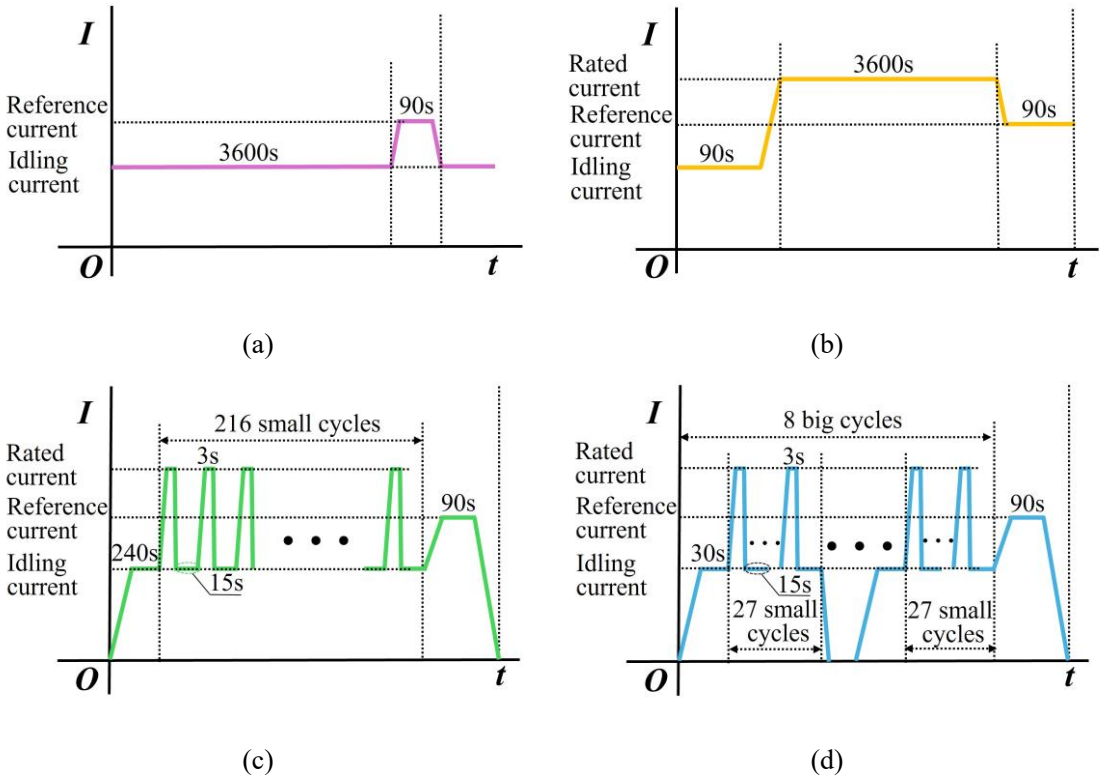

Figure 2: Test trajectory of typical operating conditions: (a) idling, (b) high-power, (c) load changing, (d) start-stop.

3 Method

3.1 Linear regression

Since the lower frequency of data acquisition, this study adopts the linear regression model to present the voltage degradation of the PEMFC. The formula for the linear regression model is as follows:

$$y=ax+b \tag{1}$$

where a denotes the slope of the model, the absolute value of which represents the voltage degradation rate. In addition, the coefficient of determination (R^2) is utilized to characterize the stability of the voltage degradation, the expression of which is shown as follows:

$$R^2=1-\frac{\sum_{i=1}^{n}(y_i-\hat{y}_i)^2}{\sum_{i=1}^{n}(y_i-\bar{y}_i)^2} \tag{2}$$

where n denotes the total number of instances; y_i, $\hat{y}_i$ and $\bar{y}_i$ denote the actual value, the fitted value, and the average of fitted values respectively.

3.2 CVM consistency

Regarding the complexity of PEMFC stack behavior during load-changing and start-stop condition tests, the cell voltage monitoring (CVM) consistency is employed to quantify single-cell voltage non-uniformity inside the stack. Figure 3 presents the CVM performance of the stack under 0H polarization testing, where 0H means the optimal condition state established through sensitivity analysis. In this study, the superior CVM consistency corresponds to a narrower voltage differential between the highest and lowest single-cell voltages.

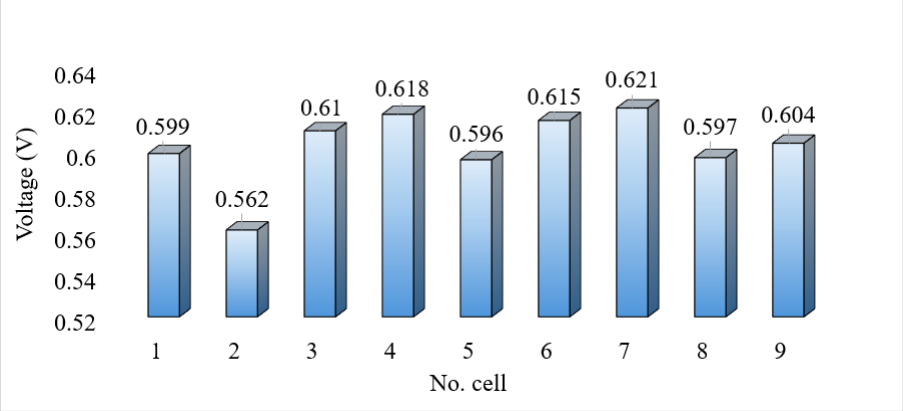

Figure 3: CVM result of the stack under 0H polarization test.

4 Results and Discussion

4.1 Idling and high-power results

Figure 4 presents the optimal average voltage results of five idling condition tests across temperature variations, the details of which are provided in Table 2. There is a significant voltage reduction during idling condition tests and the minimum degradation rate is 0.0031 V/h when the test temperature is at 60℃. Besides, the linear regression analysis demonstrates a strong correlation as the minimum R^2 is 95.17%, which indicates the stable voltage decline patterns across all tests. In addition, the proposed test shows 70℃ as the optimal temperature for idling conditions, the improvements in average voltage are 1.85%, 0.14%, 0.85%, 1.99%, and 3.84% compared to 60℃, 65℃, 75℃, 80℃ and 85℃ respectively.

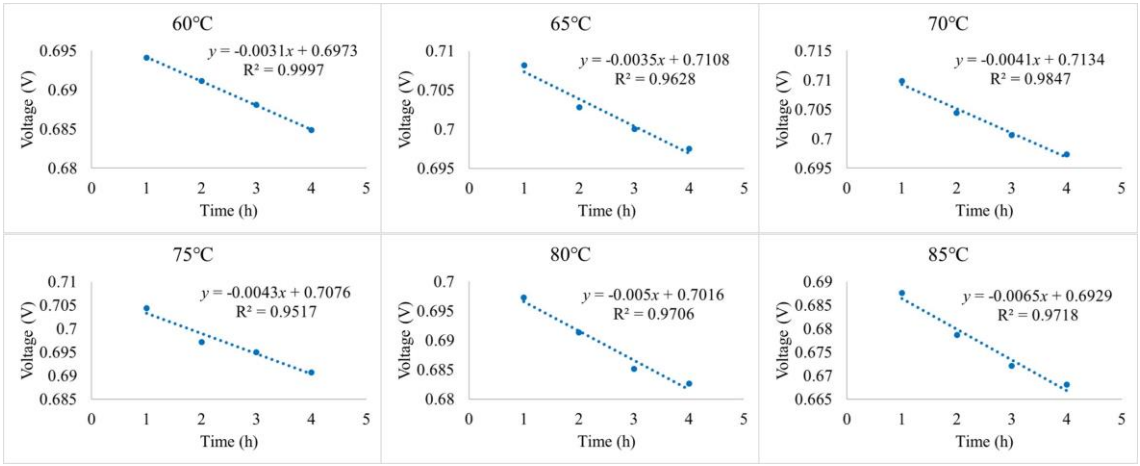

Figure 4: Trend diagram of voltage results under idling condition tests.

Figure 5 presents the optimal average voltage from five high-power condition tests across temperatures, the details of which are also provided in Table 2. There are two lower R^2 values of the linear fitting method corresponding to 68.10% and 81.56% when the high load condition tests are processed at 60℃ and 80℃, this voltage fluctuation is caused by internal water or thermal imbalances during high-power conditions. In addition, the proposed test show that 70℃ is also the optimal temperature for high-power conditions, where the voltage improvements are 3.01%, 0.68%, 1.78%, 3.01%, and 3.56% higher average voltages than 60℃, 65℃, 75℃, 80℃, and 85℃ respectively. Notably, the high-power condition tests achieve 3.96% greater average voltage than idling condition tests due to enhanced catalyst activity and gas diffusion under higher current loads.

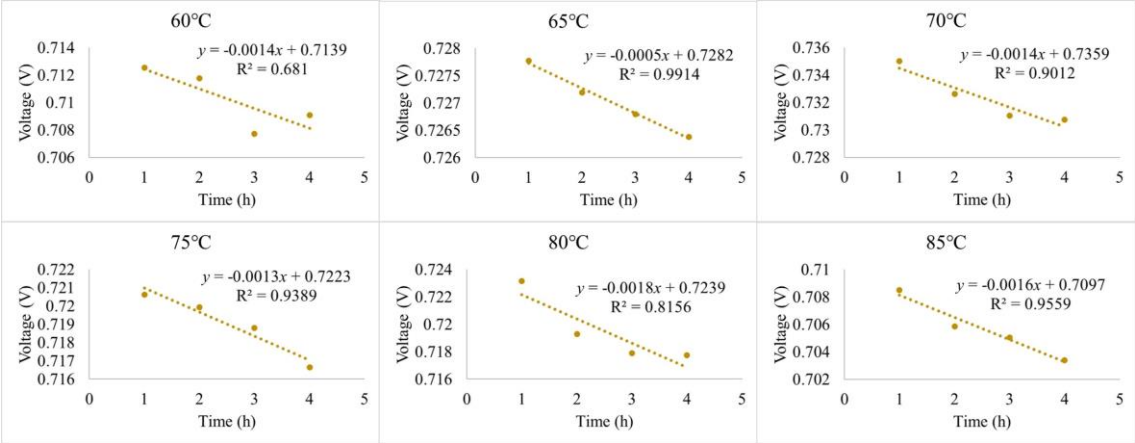

Figure 5: Trend diagram of voltage results under high-power condition tests.

Table 2 Result of idling and high-power condition tests under different temperatures

Temperature (°C)		60	65	70	75	80	85
Idling	Degradation rate (V/h)	0.0031	0.0035	0.0035	0.0043	0.0050	0.0065
	R^2 of degradation rate (%)	99.97	96.28	98.47	95.17	97.06	97.18
	Average cell voltage value (V)	0.690	0.702	0.703	0.697	0.689	0.676
	Decline of the best average value (%)	1.85	0.14	-	0.85	1.99	3.84
High load	Degradation rate (V/h)	0.0014	0.0005	0.0014	0.0013	0.0018	0.0016
	R^2 of degradation rate (%)	68.10	99.14	90.12	93.89	81.56	95.59
	Average cell voltage value (V)	0.710	0.727	0.732	0.719	0.720	0.706
	Decline of the best average value (%)	3.01	0.68	-	1.78	3.01	3.56

4.2 Load-changing and start-stop results

Figure 6 presents the average voltage under different temperatures of load-changing condition tests. Analysis reveals significant single-cell voltage variations during load-changing conditions, which prompts the use of CVM consistency as a key performance index. Figure 8 (a) presents the optimal CVM consistency results, all the details are shown in Table 3. Results show that 65℃ is the best temperature for load-changing conditions, where the minimum CVM error is 0.033 V, and the CVM consistency improvements of 112.12%, 51.52%, 121.21%, 57.58%, and 3.03% over 60℃, 70℃, 75℃, 80℃, and 85℃ respectively. Besides, the improvement in average voltage of the load-changing condition tests under 65℃ is 3.29%, 0.43%, 1.71%, 2.00%, and 1.71% higher than other tested temperatures.

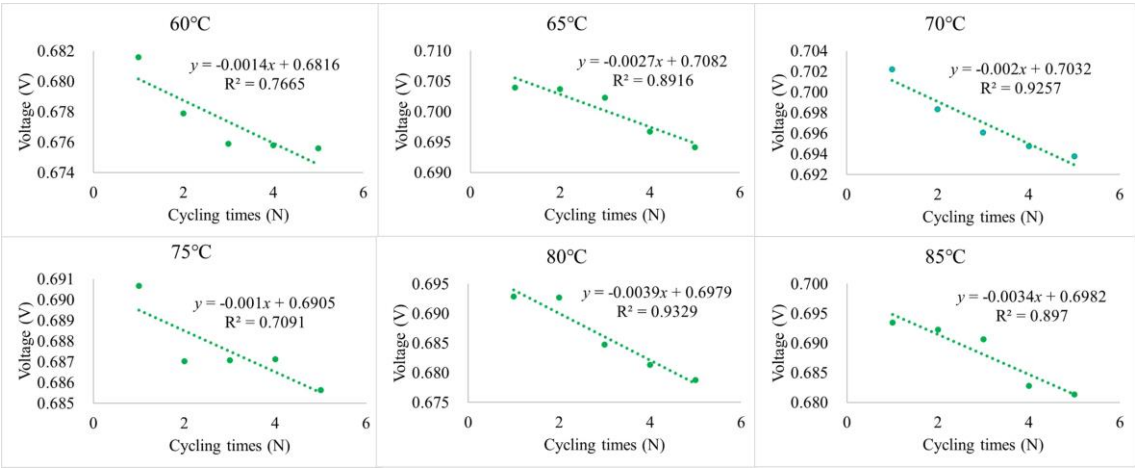

Figure 6: Trend diagram of voltage results under load-changing condition tests.

Figure 7 presents the average voltage performance of the PEMFC stack during start-stop conditions across different temperatures, while Figure 8 (b) presents the corresponding optimal CVM consistency results, all the details are shown in Table 3. Results show that 65℃ is also the best temperature for start-stop conditions, where the minimum CVM error is 0.048 V, and the CVM consistency improvements of 18.75%, 33.33%, 4.17%, 16.67%, and 29.17% over 60℃, 70℃, 75℃, 80℃, and 85℃ respectively. Besides, the improvement in average voltage of the start-stop condition tests under 65℃ is 0.98%, 0.14%, 1.40%, 3.08%, and 4.20% higher than other tested temperatures. In addition, the start-stop condition demonstrates a 2% voltage advantage compared to the load-changing condition tests under the same loading conditions, which is caused by the recovery effect during cycling.

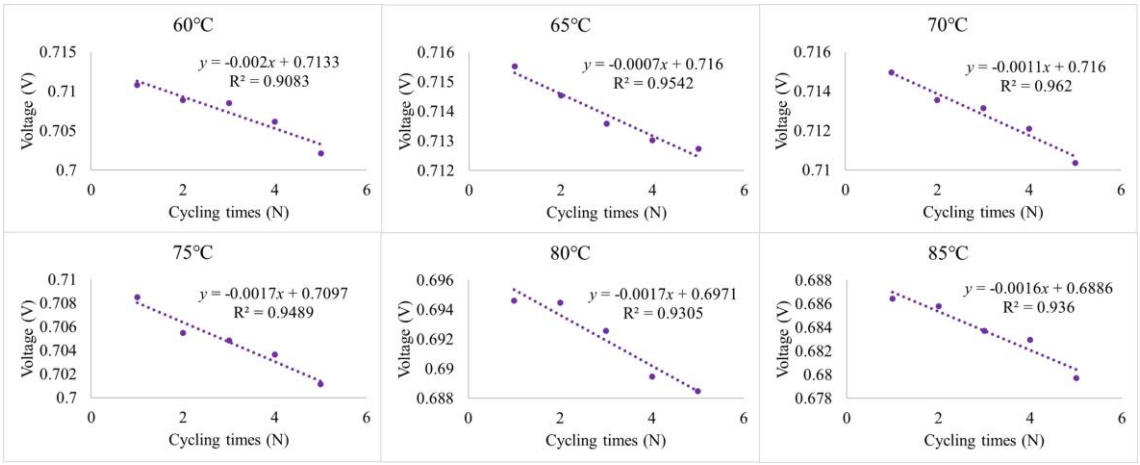

Figure 7: Trend diagram of voltage results under start-stop condition tests.

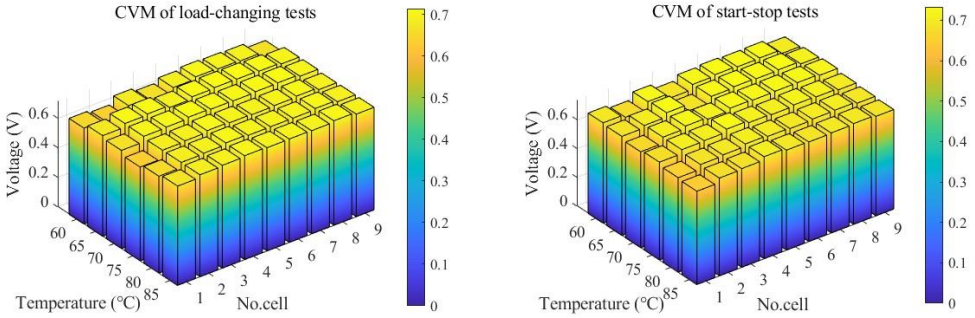

(a) (b)

Figure 8: Best CVM consistency results among five tests corresponding to different temperatures: (a) load changing, (b) start-stop.

Table 3 Result of load-changing and start-stop condition tests under different temperatures

Temperature (℃)		60	65	70	75	80	85
Load-changing	Degradation rate (V/cycle)	0.0014	0.0027	0.0020	0.0010	0.0039	0.0034
	Min error of CVM (V)	0.070	0.033	0.050	0.073	0.052	0.034
	Decline of CVM consistency (%)	112.12	-	51.52	121.21	57.58	3.03
	Average cell voltage value (V)	0.677	0.700	0.697	0.688	0.686	0.688
	Decline of the best average value (%)	3.29	-	0.43	1.71	2.00	1.71
Start-stop	Degradation rate (V/cycle)	0.0020	0.0007	0.0011	0.0017	0.0017	0.0016
	Min error of CVM (V)	0.057	0.048	0.064	0.050	0.056	0.062
	Decline of CVM consistency (%)	18.75	-	33.33	4.17	16.67	29.17
	Average cell voltage value (V)	0.707	0.714	0.713	0.704	0.692	0.684
	Decline of the best average value (%)	0.98	-	0.14	1.40	3.08	4.20

5 Conclusion

According to the actual operation requirements of the vehicle PEMFC stack, a voltage-based test including idling, high-power, load-changing, and start-stop is designed in this study, where the tests are carried out in the temperature range of [60, 65, 70, 75, 80, 85] ℃ respectively. Based on the analysis result, the conclusions drawn from this research are summarized as follows:

The test results show that 70℃ is the best operating temperature for idling and high-power conditions, where the average voltage of idling conditions increases by 1.85%-3.84% compared to 60℃, 65℃, 75℃, 80℃, and 85℃ respectively, and the average voltage of high-power conditions is increased by 0.68%-3.56%. It is worth noting that despite the similar loading modes, the optimal average voltage of the idling condition is 3.96% higher than the high-power condition.

For load-changing and start-stop conditions, the stack performs best at 65℃, where the average voltage under load-changing conditions increases by 0.43%-3.29% compared to 60℃, 65℃, 75℃, 80℃, 85℃ respectively, and the average voltage of start-stop conditions is increased by 0.14%-4.20%. Due to the recovery effect of the start-stop process, the optimal average voltage of the start-stop condition is 2% higher than the load-changing conditions under the same mode.

Regarding the CVM consistency results for the load-changing and start-stop conditions, the best temperature is still 65℃, where the improvement is 0.43%-3.29% under load-changing conditions and 0.14%-4.20% under start-stop conditions compared to 60℃, 65℃, 75℃, 80℃, 85℃ respectively.

Acknowledgment

This work was supported by the National Research Foundation of Korea (NRF) grant funded by the Korea government (MSIT) (RS-2024-00353106).

Referencing

[1] M. Perčić, N. Vladimir, I. Jovanović, and M. Koričan, “Application of fuel cells with zero-carbon fuels in short-sea shipping,” *Appl. Energy*, vol. 309, p. 118463, Mar. 2022, doi: 10.1016/j.apenergy.2021.118463.

[2] S. Fu, D. Zhang, S. W. Cha, I. Chang, G. Tian, and C. Zheng, “An extreme gradient boosting-based thermal management strategy for proton exchange membrane fuel cell stacks,” *J. Power Sources*, vol. 558, p. 232617, Feb. 2023, doi: 10.1016/j.jpowsour.2022.232617.

[3] Q. Li, Z. Liu, Y. Sun, S. Yang, and C. Deng, “A Review on Temperature Control of Proton Exchange Membrane Fuel Cells,” *Processes*, vol. 9, no. 2, Art. no. 2, Feb. 2021, doi: 10.3390/pr9020235.

[4] M. Marrony, R. Barrera, S. Quenet, S. Ginocchio, L. Montelatici, and A. Aslanides, “Durability study and lifetime prediction of baseline proton exchange membrane fuel cell under severe operating conditions,” *J. Power Sources*, vol. 182, no. 2, pp. 469–475, Aug. 2008, doi: 10.1016/j.jpowsour.2008.02.096.

[5] H. Tang, Z. Qi, M. Ramani, and J. F. Elter, “PEM fuel cell cathode carbon corrosion due to the formation of air/fuel boundary at the anode,” *J. Power Sources*, vol. 158, no. 2, pp. 1306–1312, Aug. 2006, doi: 10.1016/j.jpowsour.2005.10.059.

[6] G. Wang, F. Huang, Y. Yu, S. Wen, and Z. Tu, “Degradation behavior of a proton exchange membrane fuel cell stack under dynamic cycles between idling and rated condition,” *Int. J. Hydrog. Energy*, vol. 43, no. 9, pp. 4471–4481, Mar. 2018, doi: 10.1016/j.ijhydene.2018.01.020.

[7] Y. Shao, G. Yin, and Y. Gao, “Understanding and approaches for the durability issues of Pt-based catalysts for PEM fuel cell,” *J. Power Sources*, vol. 171, no. 2, pp. 558–566, Sep. 2007, doi: 10.1016/j.jpowsour.2007.07.004.

[8] E. F. Holby and D. Morgan, “Application of Pt nanoparticle dissolution and oxidation modeling to understanding degradation in PEM fuel cells,” *J. Electrochem. Soc.*, vol. 159, no. 5, p. B578, 2012, doi: 10.1021/acsenergylett.6b00644.

[9] T. Chu et al., “Experimental study of the influence of dynamic load cycle and operating parameters on the durability of PEMFC,” Energy, vol. 239, p. 122356, Jan. 2022, doi: 10.1016/j.energy.2021.122356.

[10] P. Pei, Q. Chang, and T. Tang, “A quick evaluating method for automotive fuel cell lifetime,” *Int. J. Hydrog. Energy*, vol. 33, no. 14, pp. 3829–3836, Jul. 2008, doi: 10.1016/j.ijhydene.2008.04.048.

[11] A. Taniguchi, T. Akita, K. Yasuda, and Y. Miyazaki, “Analysis of degradation in PEMFC caused by cell reversal during air starvation,” *Int. J. Hydrog. Energy*, vol. 33, no. 9, pp. 2323–2329, May 2008, doi: 10.1016/j.ijhydene.2008.02.049.

[12] H. Chen, X. Zhao, T. Zhang, and P. Pei, “The reactant starvation of the proton exchange membrane fuel

cells for vehicular applications: A review," *Energy Convers. Manag*., vol. 182, pp. 282–298, Feb. 2019, doi: 10.1016/j.enconman.2018.12.049.
[13] F. Nandjou, J.-P. Poirot-Crouvezier, M. Chandesris, J.-F. Blachot, C. Bonnaud, and Y. Bultel, "Impact of heat and water management on proton exchange membrane fuel cells degradation in automotive application," *J. Power Sources*, vol. 326, pp. 182–192, Sep. 2016, doi: 10.1016/j.jpowsour.2016.07.004.
[14] G. Zhang, H. Yuan, Y. Wang, and K. Jiao, "Three-dimensional simulation of a new cooling strategy for proton exchange membrane fuel cell stack using a non-isothermal multiphase model," *Appl. Energy*, vol. 255, p. 113865, Dec. 2019, doi: 10.1016/j.apenergy.2019.113865.
[15] V. A. Raileanu Ilie, S. Martemianov, and A. Thomas, "Investigation of the local temperature and overheat inside the membrane electrode assembly of PEM fuel cell," *Int. J. Hydrog. Energy*, vol. 41, no. 34, pp. 15528–15537, Sep. 2016, doi: 10.1016/j.ijhydene.2016.04.103.
[16] P. Pei and H. Chen, "Main factors affecting the lifetime of Proton Exchange Membrane fuel cells in vehicle applications: A review," *Appl. Energy*, vol. 125, pp. 60–75, Jul. 2014, doi: 10.1016/j.apenergy.2014.03.048.
[17] H.-S. Oh et al., "On-line mass spectrometry study of carbon corrosion in polymer electrolyte membrane fuel cells," *Electrochem. Commun*., vol. 10, no. 7, pp. 1048–1051, Jul. 2008, doi: 10.1016/j.elecom.2008.05.006.
[18] M. Dhimish, R. G. Vieira, and G. Badran, "Investigating the stability and degradation of hydrogen PEM fuel cell," *Int. J. Hydrog. Energy*, vol. 46, no. 74, pp. 37017–37028, Oct. 2021, doi: 10.1016/j.ijhydene.2021.08.183.
[19] J. Han, J. Han, and S. Yu, "Experimental analysis of performance degradation of 3-cell PEMFC stack under dynamic load cycle," *Int. J. Hydrog. Energy*, vol. 45, no. 23, pp. 13045–13054, Apr. 2020, doi: 10.1016/j.ijhydene.2020.02.215.
[20] S. Kang and K. Min, "Dynamic simulation of a fuel cell hybrid vehicle during the federal test procedure-75 driving cycle," *Appl. Energy*, vol. 161, pp. 181–196, Jan. 2016, doi: 10.1016/j.apenergy.2015.09.093.
[21] ChinaAutoRegs, Performance Test Methods for Fuel Cell System, GB/T 24554-2022, 2022.

Presenter Biography

Shengxiang Fu received M. S. degree from Shenyang University of Technology in 2023. He is currently pursuing a Ph.D. degree at the Department of Mechanical Engineering, Hanyang University. His research interest includes the control of PEM fuel cell systems, especially the machine learning application in the health management of PEM fuel cells.